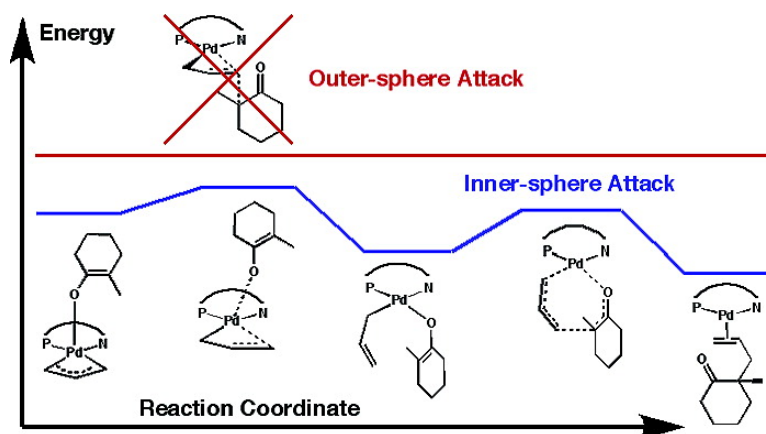


## The Inner-Sphere Process in the Enantioselective Tsuji Allylation Reaction with (*S*)-*t*-Bu-phosphinoxazoline Ligands

John A. Keith, Douglas C. Behenna, Justin T. Mohr, Sandy Ma, Smaranda C. Marinescu, Jonas Oxgaard, Brian M. Stoltz, and William A. Goddard

*J. Am. Chem. Soc.*, **2007**, 129 (39), 11876-11877 • DOI: 10.1021/ja070516j • Publication Date (Web): 08 September 2007

Downloaded from <http://pubs.acs.org> on February 14, 2009



### More About This Article

Additional resources and features associated with this article are available within the HTML version:

- Supporting Information
- Links to the 5 articles that cite this article, as of the time of this article download
- Access to high resolution figures
- Links to articles and content related to this article
- Copyright permission to reproduce figures and/or text from this article

[View the Full Text HTML](#)

## The Inner-Sphere Process in the Enantioselective Tsuji Allylation Reaction with (*S*)-*t*-Bu-phosphinooxazoline Ligands

John A. Keith,<sup>‡</sup> Douglas C. Behenna,<sup>†</sup> Justin T. Mohr,<sup>†</sup> Sandy Ma,<sup>†</sup> Smaranda C. Marinescu,<sup>†</sup> Jonas Oxgaard,<sup>‡</sup> Brian M. Stoltz,<sup>\*,†</sup> and William A. Goddard, III<sup>\*,‡</sup>

Division of Chemistry and Chemical Engineering, California Institute of Technology, Pasadena, California 91125, and Materials and Process Simulation Center (139-74), California Institute of Technology, Pasadena, California 91125

Received January 26, 2007; Revised Manuscript Received June 18, 2007; E-mail: stoltz@caltech.edu; wag@wag.caltech.edu

Challenges in natural product and pharmaceutical synthesis have fueled the development of asymmetric homogeneous catalysis in organometallic chemistry for decades.<sup>1</sup> In particular, the synthesis of enantioenriched quaternary stereocenters without stoichiometric chiral reagents remains an active area of research.

Recently, we described a method for the preparation of quaternary stereocenters of high ee (Scheme 1)<sup>2</sup> based on an enantioselective version of the general Tsuji decarboxylative allylation.<sup>3a</sup> The general allylation process involves oxidative addition to an enol carbonate (e.g., **1**) by a Pd(0) complex. The resulting allylated Pd(II) complex then reacts with ketone enolates with high regiochemical fidelity to form enantioenriched  $\alpha$ -quaternary ketones (e.g., **2**).

We reported a series of Pd catalysts that perform enantioselective allylation to form quaternary stereocenters from unstabilized prochiral enolates and non-prochiral allyl fragments.<sup>2</sup> In general, these 2-alkyl-2-allyl cyclohexanone products are distinct from the majority of asymmetric allylic alkylation products. In contrast to previous works,<sup>1c,3,4</sup> this method has allowed the regioselective allylation of hard enolates derived from ketones having two or more  $\alpha$ -acidic sites. Furthermore, a variety of enolate precursors can be employed in these reactions (i.e., enol carbonates, silyl-enol ethers, and  $\beta$ -ketoesters).

Using the (*S*)-*t*-Bu-phosphinooxazoline (PHOX) ligand,<sup>5</sup> allylated products form in high yields (80–99%) and enantiomeric excess (79–92%) with a variety of hard enolates. These ee's are reduced to negligible levels when soft enolates are utilized. Solvent effects do not seem to play a crucial role in the enantioselectivity of the reaction.<sup>6</sup> While this level of enantioselectivity is useful for many applications, it would be valuable to achieve ee's above 95%. Substantial efforts have not achieved this, prompting us to investigate mechanistic details.<sup>7</sup>

The observation that the reaction gives consistent levels of enantioselectivity regardless of the enolate precursor utilized to generate a particular product<sup>2,8</sup> suggested that these variants share a common intermediate. We obtained an X-ray crystal structure for a synthetic Pd(II)–allyl complex **3**·PF<sub>6</sub> and found that it is a viable catalytic precursor to the enantioselective decarboxylative allylation reaction.<sup>9</sup> This suggested to us that the allylated complex (**3**, Figure 1) is a likely intermediate in the reaction, and thus **3-enolate** (Scheme 2) is an intermediate as well.

Two unpublished experiments within our group suggested that we consider just one Pd<sup>0</sup>(PHOX) complex in our investigation of the mechanism: (1) experiments demonstrated a linear relationship between the ee of the catalyst and the ee of the product; and (2) simple kinetic studies showed that the reaction was first order in Pd<sup>0</sup>(PHOX) and zero order in starting material. We used quantum chemistry calculations to investigate possible mechanisms for the reaction presented in Scheme 2 starting from intermediate **3-enolate**.

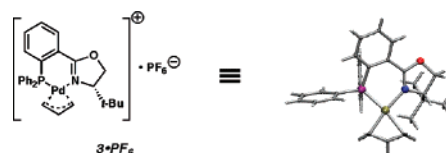
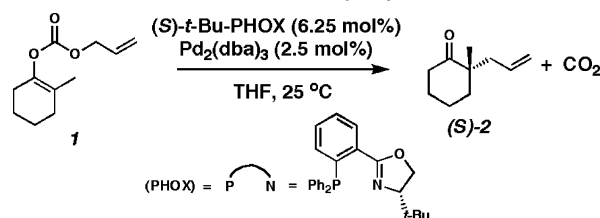
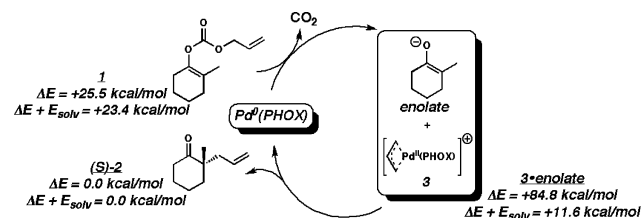


Figure 1. **3**·PF<sub>6</sub>: X-ray crystal structure for  $\pi$ -allyl complex **3**, with PF<sub>6</sub><sup>−</sup> as the counterion.

### Scheme 1. The Enantioselective Tsuji Allylation Reaction



### Scheme 2. The Enantioselective Tsuji Allylation Mechanism Studied in This Work<sup>10</sup>



All calculations<sup>11</sup> we report in this study employ the B3LYP hybrid flavor of density functional theory (DFT) that has been established to provide the most accurate energetics of the common methods using Jaguar version 6.5.<sup>15</sup>

The lowest energy conformer for intermediate **3-enolate** is a five-coordinate square pyramidal structure, **4** (Figure 2). We found that a multitude of external attack pathways lead to similar energetics, and the two lowest in energy are **6** (*trans*-P attack) and **7** (*trans*-N attack). Neither stereochemistry nor conformation of the allyl fragment (*endo* or *exo*) has a significant effect on these barriers.

We also considered an inner-sphere mechanism that converts **4** to the square planar intermediate **8** via a trigonal bipyramidal transition state **5**. We presumed that **8** could then form products through an internal C–C coupling mechanism.

Most interesting is that we find an inner-sphere mechanism that is 2.6 kcal/mol lower than that for the external attack in the gas phase and 1.6 kcal/mol lower in THF solvent (Figure 2).

A second interesting result is that reductive elimination can occur from **8** to form the  $\eta$ -2-coordinated product, **10**, through a seven-centered transition state (similar to the thermally facile Claisen rearrangement),<sup>16</sup> **9**, rather than the standard three-centered elimination analogue.<sup>17</sup> **9** is 7.0 kcal/mol lower than **5** in the gas phase and 2.5 kcal/mol lower in THF (Figure 2).

<sup>†</sup> Division of Chemistry and Chemical Engineering.

<sup>‡</sup> Materials and Process Simulation Center.

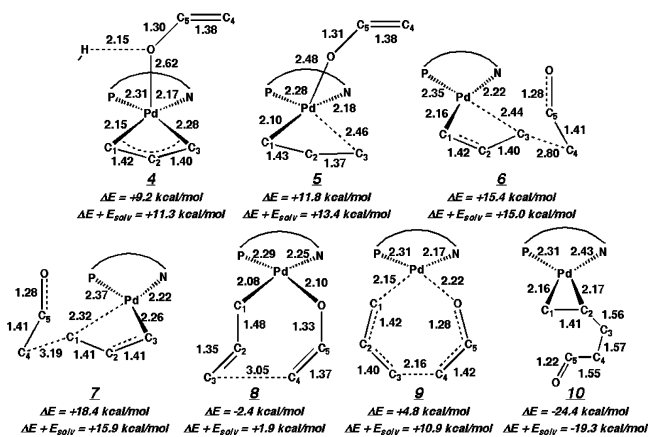


**Figure 2.** Relevant internal coordinates (Å) and thermodynamic energies of intermediates and transition states in this study. Some atoms from the enolate and PHOX ligand are omitted from the figures for clarity.

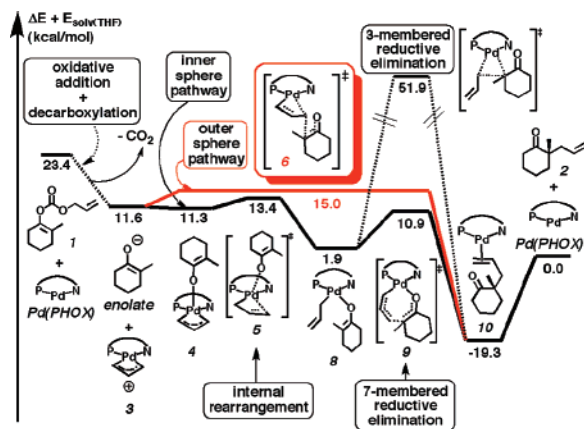


**Figure 3.** Summary of energy pathway  $\Delta E + E_{\text{solv}}$  (solvent = THF) for the enantioselective Tsuji allylation reaction.

Overall, these results contradict previous asymmetric allylic alkylation results involving soft enolate nucleophiles, prochiral allyl fragments, and Pd(PHOX) complexes that have been determined to proceed through external attack.<sup>3c,i,j</sup> Indeed, this mechanism explains how high ee's can be obtained without prochiral allyl fragments. These computational results constitute strong evidence of an inner-sphere mechanism in the Tsuji allylation reaction and may shed greater light on the details of similar inner-sphere processes already reported in the literature, especially those involving allyl-allyl type couplings.

Thus far, we have not satisfactorily identified the enantiodetermining step of this reaction. Our current results suggest that a concerted process forms products directly from **4** to **10**, but we have not ruled out stepwise transition states **5** and **9**. Figure 3 summarizes our calculated data.

**Acknowledgment.** We thank K. Tani, A. Harned, J. Enquist, and N. Sherden for experimental collaboration and discussion, and M. Day and L. Henling for crystallography assistance. J.A.K. thanks R. (Smith) Nielsen for discussions. This research was partly funded by Chevron-Texaco, and the facilities used were funded by grants from ARO-DURIP, ONR-DURIP, IBM-SUR, Fannie and John Hertz Foundation (D.C.B.), and Eli Lilly (J.T.M.) with additional support from NSF (CTS-0608889, WAG) and NIH-NIGMS (R01GM080269-01, BMS).

**Supporting Information Available:** Additional discussion of experiments, X-ray crystal and calculated molecular structures, calculated

energies, DFT functional comparisons. This material is available free of charge via the Internet at <http://pubs.acs.org>.

## References

- (1) (a) *Applied Homogeneous Catalysis with Organometallic Compounds: A Comprehensive Handbook in Three Volumes*; Cornils, B., Herrmann, W. A., Eds.; Wiley-VCH: Weinheim, Germany, 2002. (b) *Comprehensive Asymmetric Catalysis*; Jacobsen, E. N., Pfaltz, A., Yamamoto, H., Eds.; Springer: New York, 1999. (c) Pfaltz, A.; Lautens, M. In *Comprehensive Asymmetric Catalysis*; Jacobsen, E. N., Pfaltz, A., Yamamoto, H., Eds.; Springer: New York 1999; Vol. 2, pp 833–884.
- (2) Behenna, D. C.; Stoltz, B. M. *J. Am. Chem. Soc.* **2004**, *126*, 15044–15045.
- (3) (a) Tsuji, J.; Minami, I. *Acc. Chem. Res.* **1987**, *20*, 140–145. (b) Helmchen, G. *J. Organomet. Chem.* **1999**, *576*, 203–214. (c) Steinhagen, H.; Reggelin, M.; Helmchen, G. *Angew. Chem., Int. Ed.* **1997**, *36*, 2108–2110. (d) Trost, B. M. *Acc. Chem. Res.* **1996**, *29*, 355–364. (e) Trost, B. M. *Chem. Pharm. Bull.* **2002**, *50*, 1–14. (f) Trost, B. M.; Schroeder, G. M. *Chem.—Eur. J.* **2004**, *11*, 174–184. (g) Trost, B. M. *J. Org. Chem.* **2004**, *69*, 5813–5837. (h) Trost, B. M.; Lee, C. In *Catalytic Asymmetric Synthesis*; Ojima, I., Ed.; Wiley-VCH: New York, 2000; pp 593–649. (i) Bäckvall, J.-E.; Nordberg, R. E.; Vågberg, J. *Tetrahedron Lett.* **1983**, *24*, 411–412. (j) Helmchen, G.; Steinhagen, H.; Reggelin, M.; Kudis, S. In *Selective Reactions of Metal-Activated Molecules*; Werner, H., Schreier, P., Eds.; Vieweg Verlag: Wiesbaden, Germany, 1998; pp 105–115.
- (4) Prochiral nucleophile studies: (a) Hayashi, T.; Kanehira, K.; Hagihara, T.; Kumada, M. *J. Org. Chem.* **1988**, *53*, 113–120. (b) Kuwano, R.; Ito, Y. *J. Am. Chem. Soc.* **1999**, *121*, 3236–3237. (c) Kuwano, R.; Uchida, K.; Ito, Y. *Org. Lett.* **2003**, *5*, 2177–2179. (d) Sawamura, M.; Nagata, H.; Sakamoto, H.; Ito, Y. *J. Am. Chem. Soc.* **1992**, *114*, 2586–2592.
- (5) (a) Helmchen, G.; Pfaltz, A. *Acc. Chem. Res.* **2000**, *33*, 336–345. (b) Williams, J. M. J. *Synlett* **1996**, 705–710.
- (6) See Supporting Information. For most substrates, the optimal solvent was THF (yield = 96%, ee = 88% for product (S)-**2**); however, the reaction also performed surprisingly well in a variety of nonpolar solvents, including benzene (yield = 99%, ee = 88% for product (S)-**2**).
- (7) We note that substituted allyl fragments typically used as stereochemical probes for asymmetric allylation reactions are unsuitable for our catalyst system. See Supporting Information for details.
- (8) Mohr, J. T.; Behenna, D. C.; Harned, A. M.; Stoltz, B. M. *Angew. Chem., Int. Ed.* **2005**, *44*, 6924–6927.
- (9) See Supporting Information. Crystallographic data have been deposited at the CCDC, 12 Union Road, Cambridge CB2 1EZ, UK, and copies can be obtained on request, free of charge, by quoting the publication citation and the deposition number 245187.
- (10) Pd<sup>0</sup>(PHOX) is believed to form allylated complex **3** with the concomitant decarboxylation of **1**. Thermodynamic values are calculated with respect to the uncoordinated products (S)-**2** + Pd(PHOX).  $E_{\text{solv}}$  is the energy associated with placing a gas-phase molecule in a solvent continuum and can be added to  $\Delta E$  values to obtain solvent-phase results. Other calculation results are in the Supporting Information.
- (11) Calculations are on 82-atom systems with B3LYP hybrid DFT and mixed basis set geometries (LACVP\*\* on atoms shown in Figure 3 and the MIDI! basis set on all other atoms). Single-point energies are calculated with the LACV3P\*\*++ basis set. In addition to electronic energy and thermodynamic contributions, we considered single-point solvent effects for THF (probe radius = 2.527 Å,  $\epsilon = 7.52$ ) using the Jaguar self-consistent Poisson–Boltzmann solver (ref 12) and the LACV3P\*\* basis set. Computational studies by our group show that this method leads to sufficiently accurate reaction barrier heights for large organometallic complexes, including those of palladium (ref 13). Single-point control calculations were carried out at these geometries with the PBE (ref 14) pure density functional DFT and the LACV3P\*\*++ basis set, leading to differences between critical barriers with rms = 1.2 kcal/mol.
- (12) (a) Marten, B.; Kim, K.; Cortis, C.; Friesner, R. A.; Murphy, R. B.; Ringnalda, M. N.; Sitkoff, D.; Honig, B. *J. Phys. Chem.* **1996**, *100*, 11775–11788. (b) Tannor, D. J.; Marten, B.; Murphy, R.; Friesner, R. A.; Sitkoff, D.; Nicholls, A.; Ringnalda, M.; Goddard, W. A., III; Honig, B. *J. Am. Chem. Soc.* **1994**, *116*, 11875–11882.
- (13) (a) Keith, J. A.; Oxgaard, J.; Goddard, W. A., III. *J. Am. Chem. Soc.* **2006**, *128*, 3132–3133. (b) Keith, J. M.; Nielsen, R. J.; Oxgaard, J.; Goddard, W. A., III. *J. Am. Chem. Soc.* **2005**, *127*, 13172–13179. (c) Nielsen, R. J.; Goddard, W. A., III. *J. Am. Chem. Soc.* **2006**, *128*, 9651–9660.
- (14) (a) Perdew, J. P.; Burke, K.; Ernzerhof, M. *Phys. Rev. Lett.* **1996**, *77*, 3865–3868. (b) Perdew, J. P.; Burke, K.; Ernzerhof, M. *Phys. Rev. Lett.* (erratum) **1997**, *78*, 1396.
- (15) *Jaguar*, version 6.5; Schrödinger, LLC, New York, 2005.
- (16) Lutz, R. P. *Chem. Rev.* **1984**, *84*, 205–247.
- (17) Calculations on a non-oxy analogue of this mechanism were first presented in ref 18. The transition state for the three-membered ring is very high, +46.9 in gas phase and +51.9 kcal/mol in solvent. The explanation for high barriers of C–C reductive couplings from Pd(II) is discussed in ref 19.
- (18) Méndez, M.; Cuerva, J. M.; Gómez-Bengoa, E.; Cárdenas, D. J.; Echavarran, A. M. *Chem.—Eur. J.* **2002**, *8*, 3620–3628.
- (19) (a) Low, J. J.; Goddard, W. A., III. *J. Am. Chem. Soc.* **1986**, *108*, 6115–6128. (b) Low, J. J.; Goddard, W. A., III. *Organometallics* **1986**, *5*, 609–622.

JA070516J